

AD-A037 954

ARMY ELECTRONICS COMMAND FORT MONMOUTH N J
MESOSCALE DETERMINATION OF CLOUD-TOP HEIGHT: PROBLEMS AND SOLUT--ETC(U)
MAR 77 R D LOW, J D HORN

F/G 4/2

UNCLASSIFIED

ECOM-5814

NL

1 OF 1
ADA037954

1



END

DATE
FILMED

4-77



ADA 037954

12

FG

AD

Reports Control Symbol
OSD-1366

RESEARCH AND DEVELOPMENT TECHNICAL REPORT
ECOM-5814

MESOSCALE DETERMINATION OF CLOUD-TOP HEIGHT: PROBLEMS AND SOLUTIONS

By

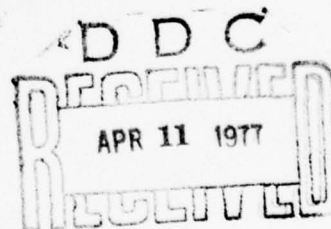
Richard D.H. Low
J.D. Horn

Atmospheric Sciences Laboratory

US Army Electronics Command
White Sands Missile Range, New Mexico 88002

March 1977

Approved for public release; distribution unlimited.



DDC FILE COPY

ECOM

UNITED STATES ARMY ELECTRONICS COMMAND - FORT MONMOUTH, NEW JERSEY 07703

NOTICES

Disclaimers

The findings in this report are not to be construed as an official Department of the Army position, unless so designated by other authorized documents.

The citation of trade names and names of manufacturers in this report is not to be construed as official Government indorsement or approval of commercial products or services referenced herein.

Disposition

Destroy this report when it is no longer needed. Do not return it to the originator.

14 REPORT DOCUMENTATION PAGE		READ INSTRUCTIONS BEFORE COMPLETING FORM	
1. REPORT NUMBER ECOM-5814	2. GOVT ACCESSION NO.	3. RECIPIENT'S CATALOG NUMBER	
4. TITLE (and Subtitle) MESOSCALE DETERMINATION OF CLOUD-TOP HEIGHT: PROBLEMS AND SOLUTIONS.		5. TYPE OF REPORT & PERIOD COVERED Research and development, technical rept.	
6. AUTHOR(s) Richard D. H. Low J. D. Horn		7. PERFORMING ORG. REPORT NUMBER	
8. PERFORMING ORGANIZATION NAME AND ADDRESS Atmospheric Sciences Laboratory White Sands Missile Range, New Mexico 88002		9. CONTRACT OR GRANT NUMBER(s)	
10. CONTROLLING OFFICE NAME AND ADDRESS US Army Electronics Command Fort Monmouth, New Jersey 07703		11. PROGRAM ELEMENT, PROJECT, TASK AREA & WORK UNIT NUMBERS DA Task 1T161101A91A	
12. MONITORING AGENCY NAME & ADDRESS (if different from Controlling Office)		13. REPORT DATE Mar 1977	
		14. NUMBER OF PAGES 38	
		15. SECURITY CLASS. (of this report) UNCLASSIFIED	
		15a. DECLASSIFICATION/DOWNGRADING SCHEDULE	
16. DISTRIBUTION STATEMENT (of this Report) Approved for public release; distribution unlimited.			
17. DISTRIBUTION STATEMENT (of the abstract entered in Block 20, if different from Report)			
18. SUPPLEMENTARY NOTES			
19. KEY WORDS (Continue on reverse side if necessary and identify by block number) Cloud-top height Satellite instrumentation Mesoscale Infrared radiative transfer Satellite imagery Blackbody			
20. ABSTRACT (Continue on reverse side if necessary and identify by block number) This report presents an overview of the problems dealing with the mesoscale determination of cloud-top height from the infrared imagery of the geostationary operational environmental satellites, the GOES series. Such problems as the blackbody assumption of clouds, the field of view of the satellite radiometer, instrument response, the presence of overlying thin cirrus clouds, gaseous absorption in the 10.5µm to 12.6µm infrared band, and the temperature-height relationships within and without the cloud as well as some solutions are discussed. These problems reduce to one of finding the true cloud temperature. It is			

next page
y/B

20. ABSTRACT (cont)

cont → argued that computer simulation of various cloudy situations by solving the radiative transfer equation for a plane parallel inhomogeneous cloud atmosphere may prove ultimately to be less costly and more effective.



ACQUISITION FOR	
NTIS	NTIS SYMBOL <input checked="" type="checkbox"/>
DDC	DDC SYMBOL <input type="checkbox"/>
UNANNOUNCED	<input type="checkbox"/>
JUSTIFICATION	
BY	
DISTRIBUTION/AVAILABILITY STATEMENT	
UNIT	APPROVAL/REVIEW
A	

CONTENTS

	<u>Page</u>
INTRODUCTION	2
MESOSCALE CONSIDERATIONS	3
METEOROLOGICAL SATELLITES AND INSTRUMENTS	4
SMS	5
ITOS VTPR SYSTEM	5
ITOS SCANNER	11
DMSP SATELLITE	11
IR TECHNIQUE AND ITS PROBLEMS	11
SOME SOLUTIONS	20
SUMMARY	21
ABBREVIATIONS	24
REFERENCES	25

INTRODUCTION

Generally speaking, the presence of clouds hampers target acquisition and air and ground operations. It would be advantageous to a field commander to have cloud information such as ceiling, amount, and top height readily available at all times, over both friendly and enemy territories. The rapid advance of satellite technology has made it possible to derive this and other information from meteorological satellite radiometric measurements in both the visible and the infrared spectral regions.

Although it is difficult to determine cloud ceiling, the techniques for deriving cloud amounts and cloud-top heights on a synoptic scale from remote sensing of underlying visible and IR radiation are fairly well established [1-8]. To determine the amount of cloud coverage is relatively simple and straightforward and it will not be dealt with. To derive the cloud-top height involves finding the so-called effective blackbody temperature from the effective upwelling radiance measured by the satellite IR radiometer and then matching this temperature with the one obtained or predicted concomitantly in both time and space from the temperature soundings. Though there are some problems [4] with these techniques, it has become more or less routine now to delineate the high, middle, and low clouds as well as the amounts of cloud coverage on a global scale, which has not heretofore been possible with conventional weather observations.

However, Army battlefield operations are not synoptic scale, but rather, mesoscale military activities. Our interest, therefore, lies in the determination of cloud parameters on a mesoscale. In mesoscale applications, the problems with these techniques are further compounded, not so much in the determination of cloud amounts, but in that of cloud-top heights, the latter being derived almost exclusively from IR imagery in the 10- μ m window region. Microwave imagery helps, but only to the extent that its great penetration power enables us to separate the cold ice- and snow-covered ground from an equally cold cloud top, one which would otherwise be indistinguishable in the visible or IR imagery.

This report proposes to give an overview of the problems in the determination of cloud tops on a mesoscale and will, for the above-mentioned reason, limit our discussions to the IR technique only. Following a brief exposition on mesoscale requirements and the type of satellites which would best meet these requirements, a short description of the satellites and their onboard instruments in current use is presented. Then, the problems with the IR technique in mesoscale application will be discussed and the solutions explored. Finally, it is argued that computer simulation may offer a more economical and efficient means to cope with some of the problems. The present report may be looked upon as the first of a series of three projected reports dealing with IR imagery in the 10- μ m window region; thus, it is labeled an overview of the IR technique. The next report considers the theoretical foundation of IR imagery and explores the

optical and radiative properties of several cloud types. The third report represents an effort to extend the theoretical foundation and link it to imagery analysis; a comparison will be carried out in a few selected cases between the radiance values obtained through numerical simulation and those observed by the satellite radiometer.

MESOSCALE CONSIDERATIONS

In military applications, the determination of cloud-top heights and amounts calls for a scale in both time and space well within the realm of mesometeorology. According to the Glossary of Meteorology [9], mesometeorology is concerned with the detection and analysis of the state of the atmosphere as it exists between meteorological stations (some 80 to 800 km apart) or at least well beyond the range of normal observation from a single point. The type of major weather phenomena that are small enough to remain undetected within a normal observational network are sometimes called "mesometeorological"; they include tornadoes, thunderstorms, and immature tropical cyclones. However, the detailed observation of larger-scale occurrences (fronts and precipitation areas) which may extend beyond 1600 km is also an important part of mesometeorology [10]. In this application the cloud parameters will be examined on a scale up to 100 by 100 km in area, up to 10 km in height, and up to 100 minutes in time.

In general, cloud systems, the visible evidence of atmospheric circulation, are synoptic scale phenomena. Their movements, and hence the changes in cloud forms, heights and amounts, are usually dictated by the prevailing large-scale patterns and cannot be divorced from synoptic analysis. Nevertheless, dramatic changes in cloud forms, heights, and amounts often take place in time intervals of the order of minutes and can therefore be treated as mesoscale phenomena. Clouds born of surface heating, land and sea circulation, mountain waves, and propagating gravity waves, though not unaffected by the prevailing synoptic patterns, are local phenomena and belong in the sphere of mesometeorology. Rapid changes of such cloud patterns can indeed occur in a matter of minutes [11] and will require frequent observations at intervals of 1 to 10 minutes since the art of mesoscale forecasting is still in its infancy.

There are essentially two major classes of satellites; those which traverse the earth from pole to pole, the so-called polar orbiters such as the NOAA [12, 13] and DMSP (Defense Meteorological Satellite Program) [14, 15] series, and those which remain stationary over some fixed point along the equator and watch the earth go by, the so-called geostationary satellites such as the SMS (Synchronous Meteorological Satellite)/GOES (Geostationary Operational Environmental Satellite) series [16]. It is not difficult to see that the former class of satellite flies over any

spot along its suborbital track no more than twice daily, once in the daytime and the other at night, somewhat like our present upper-air sounding schedule. The cloud information acquired by this type of satellite may be sufficient for synoptic application. The latter satellite, being stationary over the equator, scans the entire globe in less than 30 minutes. In other words, any dramatic changes in global weather patterns which may occur in a longer time period than 30 minutes will be captured. As a matter of fact, the satellite, on command, will scan only a limited portion of the globe; thereby reducing the scan time to perhaps a few minutes for a sector and greatly enhancing our ability to detect and track mesoscale weather changes such as severe thunderstorms and tornados, even over enemy territory. The present instrument in SMS/GOES called VISSR (Visible Infrared Spin Scan Radiometer) [17] has a fine resolution in both visible and infrared imagery (about 1 km in the visible and about 4 km in the infrared at the nadir; i.e., over the equator). An advanced version called VAS (VISSR Atmospheric Sounder), which will not only have indirect sounding capability, but also will provide additional imaging channels [18], will be introduced before the end of 1980. In mesometeorology, that the type of satellite which appears to best meet our mesoscale requirements belongs in the SMS/GOES series can no longer be questioned.

However, since the SMS/GOES is geostationary at a predesignated longitude over the equator, there will be some errors in the determination of cloud amounts and cloud-top heights over areas away from the equator, less so along the same meridian but more so at other meridians. These errors arise not only from areal distortion which makes an area at 50° latitude twice as large as an area at the equator along the same longitude [19], but also from vertical distortion in which both the top and the sides of a cloud are observed. In this respect, it would be well-advised to carry out a comparison between the cloud imagery generated by the two types of satellites.

METEOROLOGICAL SATELLITES AND INSTRUMENTS

A number of meteorological satellites provide data useful in cloud-top height estimation. These include the SMS and ATS (Applications Technology Satellite) geosynchronous satellites [16], which yield full earth pictures at half-hour intervals. Also available are the polar orbiter meteorological satellites, including the Improved Tiros Operational System (ITOS) series of spacecraft [12], the Nimbus series of experimental satellites [20, 21], and satellites from the DMSP program [14, 15]. The geosynchronous meteorological satellites provide imagery in the visible and IR bands. The polar orbiting satellites provide visible and IR imagery from scanners and temperature soundings derived from multichannel profiling radiometers [13, 14].

The following paragraphs describe sensing systems, detectors, and instrumentation available aboard the various meteorological spacecraft that have potential utility in solving the cloud height problem.

SMS

The SMS/GOES (Geostationary Operational Environmental Satellite) provides full earth images at half-hour intervals during day and nighttime hours. In 1975, SMS A was geostationary over the earth's equator at 70 W longitude, 36,000 km from earth. SMS images are telemetered to the NOAA Command and Data Acquisition (CDA) station at Wallops Island, Virginia. The computer processed data are then relayed via the satellite to the Direct Readout Ground Station (DRGS) SMS unit at WSMR.

The SMS is spin stabilized at 100 revolutions per minute about a cylindrical axis. The Visible Infrared Spin-Scan Radiometer (VISSR) unit (Fig. 1) has a side viewing 41 cm aperture that scans the earth once each revolution of the satellite. Table 1 gives design data, and Fig. 2 shows a visual depiction of SMS/GOES.

The VISSR scans the earth pole to pole in 18 minutes (1821 latitude steps, see Table 1). One full disc image is completed each half hour. This image is stored on magnetic tape and produced as a 22- by 22-inch image transparency on the DRGS laser fax system. Other combinations available include a 7.5-minute sector scan for a particular active storm area on the surface of the earth characterized by rapidly changing cloud patterns.

Later versions of SMS/GOES will use the VAS system made up of a VISSR, an atmospheric sounder, and a multispectral scanner. Another version of SMS will include a microwave scanner. The new detectors can be employed in the determination of cloud-top heights. The VAS system is designed for the 1979-1981 GOES series (SMS, F, G, and H) and the microwave sensor for the 1985 satellite [18].

ITOS VTPR SYSTEM

The Vertical Temperature Profiling Radiometer (VTPR) is a continuous day and night eight-channel radiometer sounding system aboard the ITOS spacecraft. Six of the radiometer channels are in the 15μ CO_2 absorption band (Table 2) [13]. One radiometer channel scans at a water vapor absorption band (535 cm^{-1}) and one channel is in an atmospheric window at 833 cm^{-1} . The optical system of the VTPR consists of a scanning mirror (Fig. 3), and 73.5 mm Cassegrainian telescope, a filter wheel and chopper, and a detector assembly. The detector assembly consists of an Irtran 4

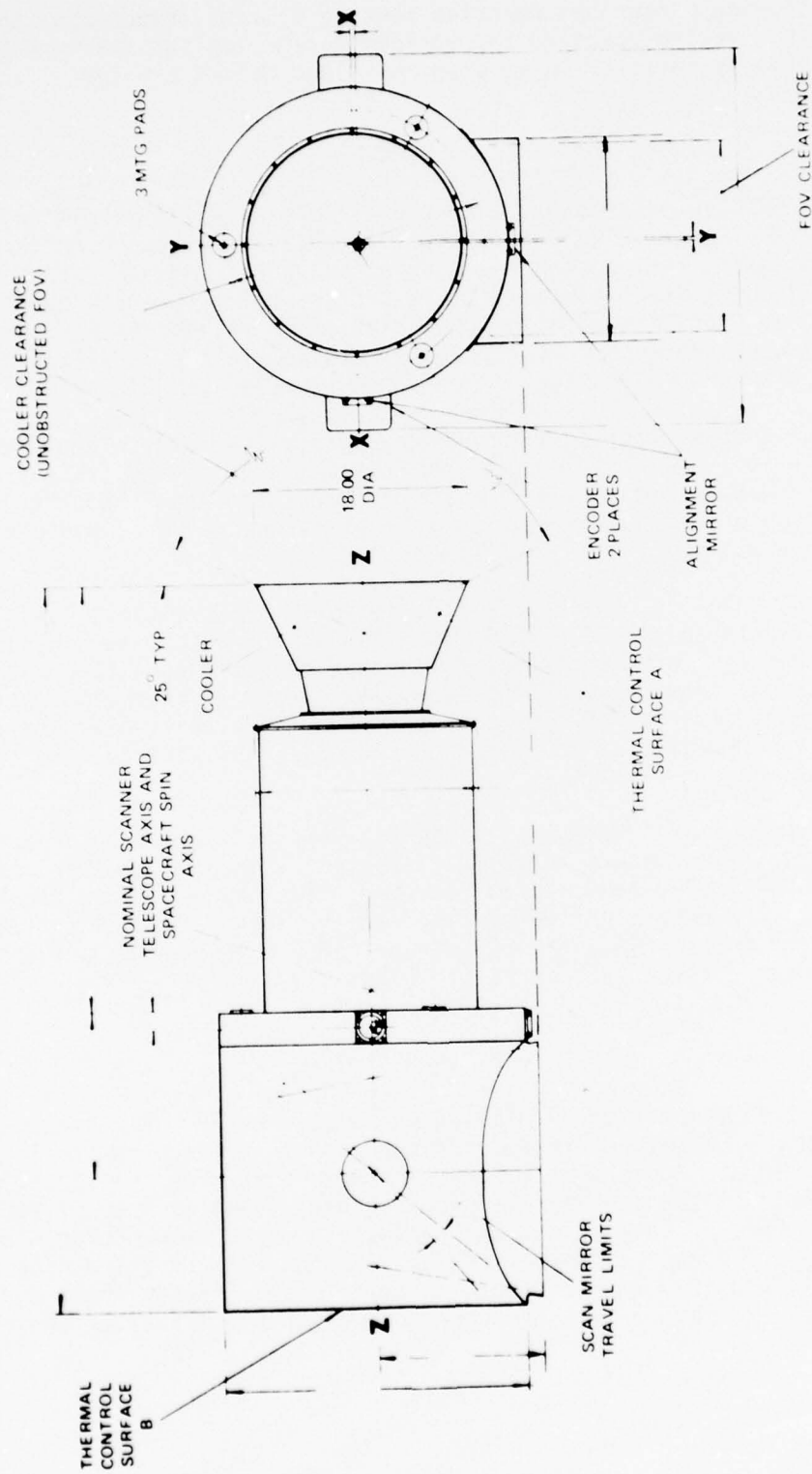


Figure 1. VISSR scanner system.

TABLE 1
DESIGN SUMMARY OF VISSR/SMS

<u>Design Parameters</u>	<u>Visible Channel</u>	<u>Thermal Channel</u>
No. of channels	8	1 plus 1 redundant
Wavelengths band of operation, half-power points	0.55-0.75 micron	10.5-12.6 microns
Instantaneous geometric field of view (IGFOV)	0.025 x 0.021 mr	0.25 x 0.25 mr
Detector	Photo multiplier tube	HgCdTe
Size	----	0.015 x 0.105 mm
Response	S-20 (enhanced)	----
Scan period	0.6 sec	0.6 sec
Dwell time	2.4×10^{-6} sec	1.9×10^{-5} sec
Information bandwidth	210 kHz	26 kHz
Dynamic range, albedo (%); target temperature ($^{\circ}$ K)	0 to 100	0 to 315
Ground resolution, nadir	0.5 nm	4.85 nm
Scan lines 1821 latitude steps		
Trace time 18.2 min		
Retrace time 1.7 min		
Frame Size $20^{\circ} \times 20^{\circ}$		
Noise Equivalent		
Radiance 0.9×10^{-5} W cm $^{-2}$ ster $^{-1}$ (HgCdTe detectors)		
Telemetry: receive 148 MHz transmit 136 MHz		
Receiver antenna gain -6.5 dB		
Transmitter antenna gain -5 dB		

TABLE 2

NOMINAL SPECTRAL INTERVALS FOR VTPR FILTERS
AND SUMMARY OF VTPR PARAMETERS

Filter No.	Filter Wheel Position	Center Wavelength (μm)	Filter Bandpass		Parameter	Nominal Value
			Half-Width (cm^{-1})	Tenth-Width (cm^{-1})		
1	1	14.96	668.5	3.5	Spectral range	12-19 μm
2	8	14.77	677.5	10	Line rate	4.8 lines/min
3	2	14.38	695.0	10	Field of view	2.136° by 2.236°
4	7	14.12	708.0	10	Dynamic range	0 to 210 $\text{mW}/(\text{m}^2 \text{ sr cm}^{-1})$
5	3	13.79	725.0	10	Sensitivity*	0.25 $\text{mW}/(\text{m}^2 \text{ sr cm}^{-1})$ or less
6	6	13.38	747.0	10	Digital signal output	16 bits
7	4	18.69	535.0	18	Data rate	256 bits/sec
8	5	11.97	833.0	10	Primary f/No.	f/3
					Effective f/No.	f/0.6 at the detector
					Scan-mirror aperture	7.6 cm

*Q-Branch 0.75 $\text{mW}/(\text{m}^2 \text{ sr cm}^{-1})$

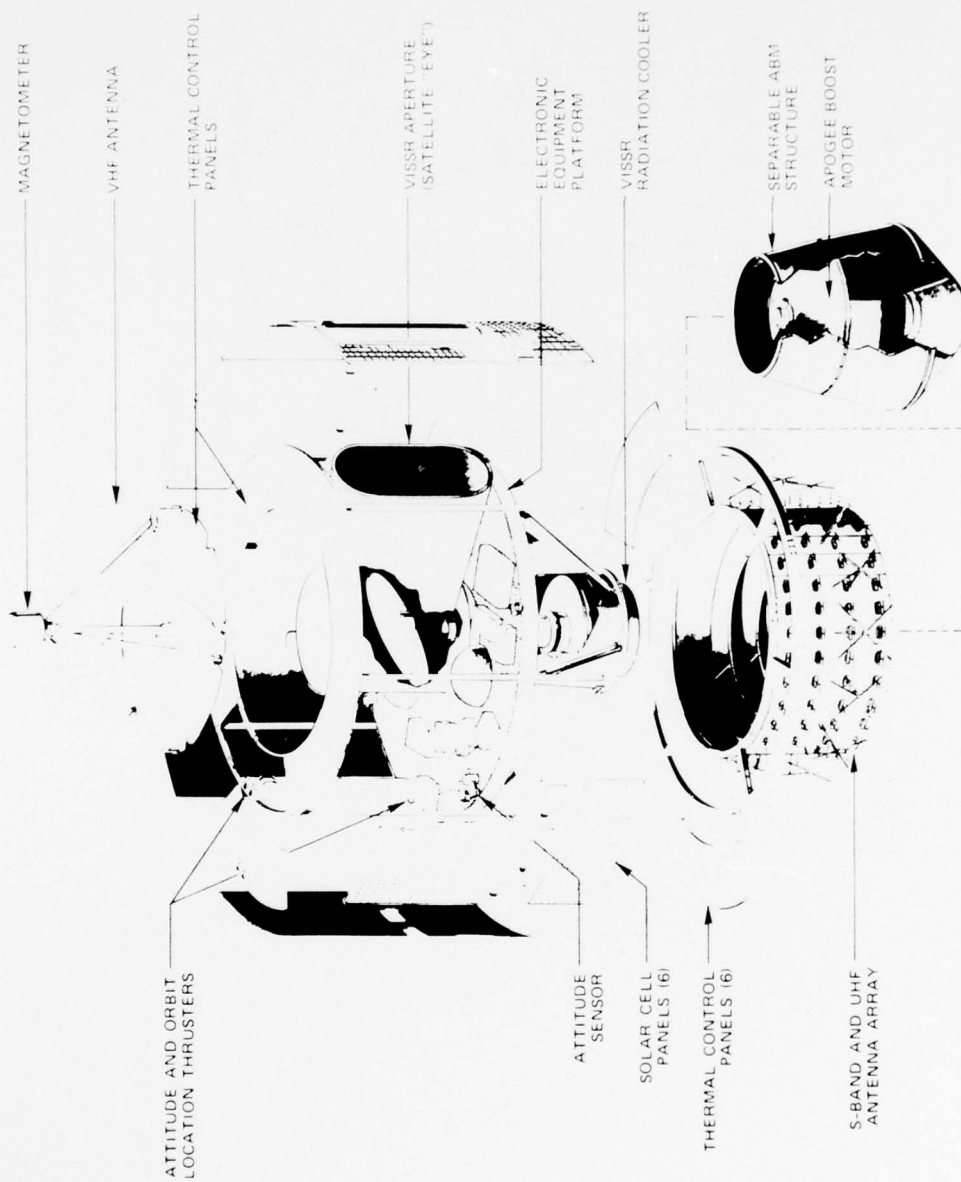
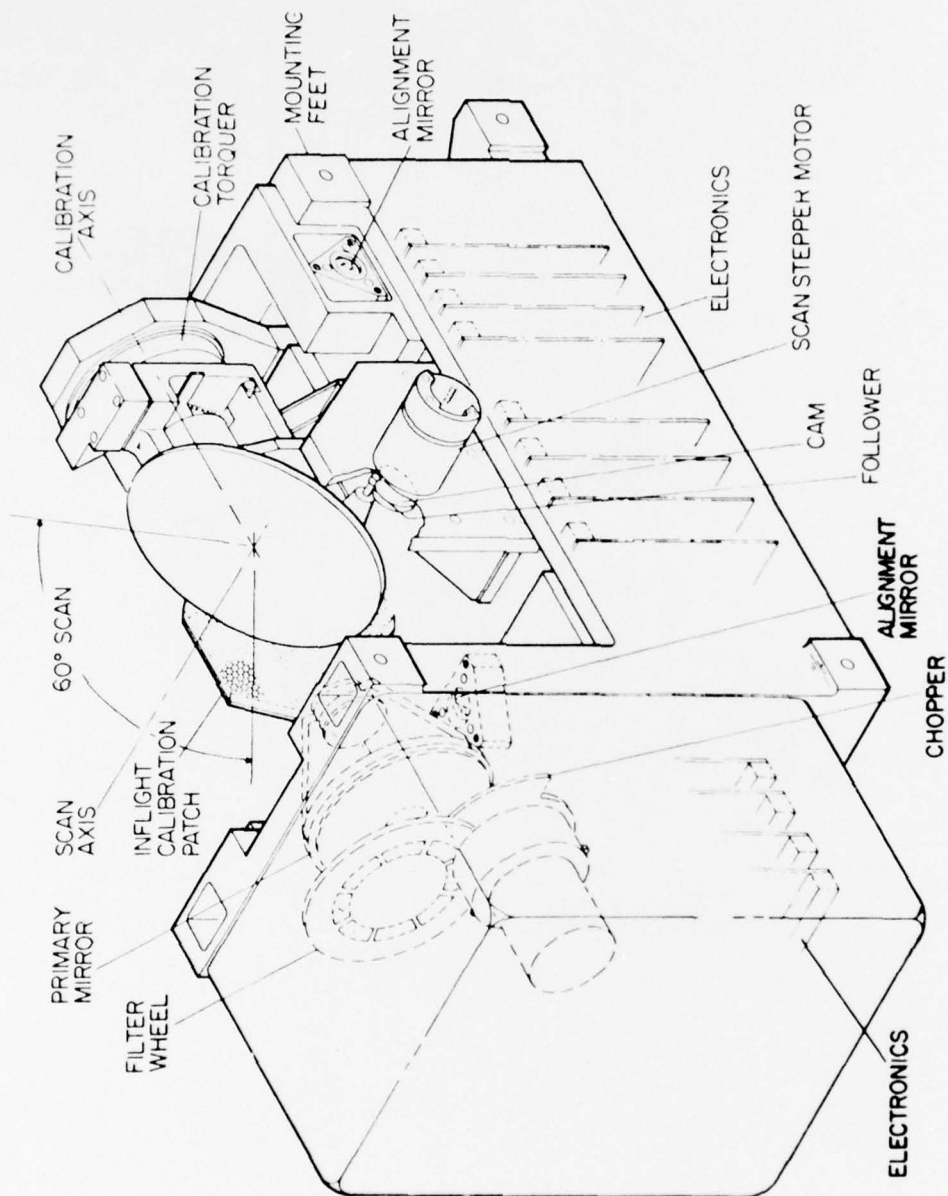


Figure 2. Satellite description SMS.



ISOMETRIC VIEW OF VTPR (Cover Removed)

Figure 3. VTPR instrument.

lens, a germanium window, and an uncooled pyroelectric detector. Radiance measurements are calibrated from 0 to $204.8 \text{ mW/m}^2 \text{ sr cm}^{-1}$. A single VTPR scan takes 12.5 seconds. A 0.5-second interval is used for each of 23 scan spots.

ITOS SCANNER

Major operating parameters of the ITOS polar orbiter meteorological satellite (Fig. 4) are shown in Table 3 [12]. The scanning radiometer (SR) subsystem of the ITOS satellite consists of two 2-channel radiometers. Each radiometer consists of a scanning unit, an electronics package, and SR processors and recorders. The two channels of the SR operate in the visible ($0.5 \mu\text{m}$ to $0.73 \mu\text{m}$) and in the IR ($10.5 \mu\text{m}$ to $12.5 \mu\text{m}$) bands. SR resolution is 2 nm for visible data and 4 nm for IR data at the subsatellite point. Later versions have resolution to 0.5 nm.

DMSP SATELLITE

The Block 5D DMSP satellite travels in a polar orbit $450 \pm 9 \text{ nm}$ above the earth. The payload of the satellite weighs 136 kg and operates at a power of 170 W. The power source is a circular track deployable solar array with storage provided by NiCd battery cells.

The visible scanner (operational line-scan system, OLS) has a resolution of 1.5 by 1.5 nm in the global scan mode and 0.3 by 0.3 nm in the very high resolution mode.

Resolution capabilities of the scanners are summarized in Table 4 [15]. The OLS (Fig. 5) [14] consists of a visible-IR Cassegrainian telescope relay optics, a three-segment silicon diode visible detector (Fig. 6) [14], and a two-segment, trimetal, HgCdTe, IR detector. The primary mirror is a 20 cm f/1.0 parabolic folded optical system.

The visual daytime response is in the 0.4μ to 1.1μ band for maximum contrast between earth, sea, and cloud elements. The IR response is in the 9μ to 13μ band for detection of both water and ice crystal clouds. The IR detector is accurate to 1°K rms between 210°K and 310°K . The noise equivalent temperature difference (NETD) is within 1°K .

IR TECHNIQUE AND ITS PROBLEMS

The theoretical basis for the determination of cloud-top temperature in the IR spectrum rests with the manipulation of the radiative transport equation [22, 23]. The amount of radiance detected by the SMS IR radiometer comes mainly from the thermal emission of liquid and solid aerosol

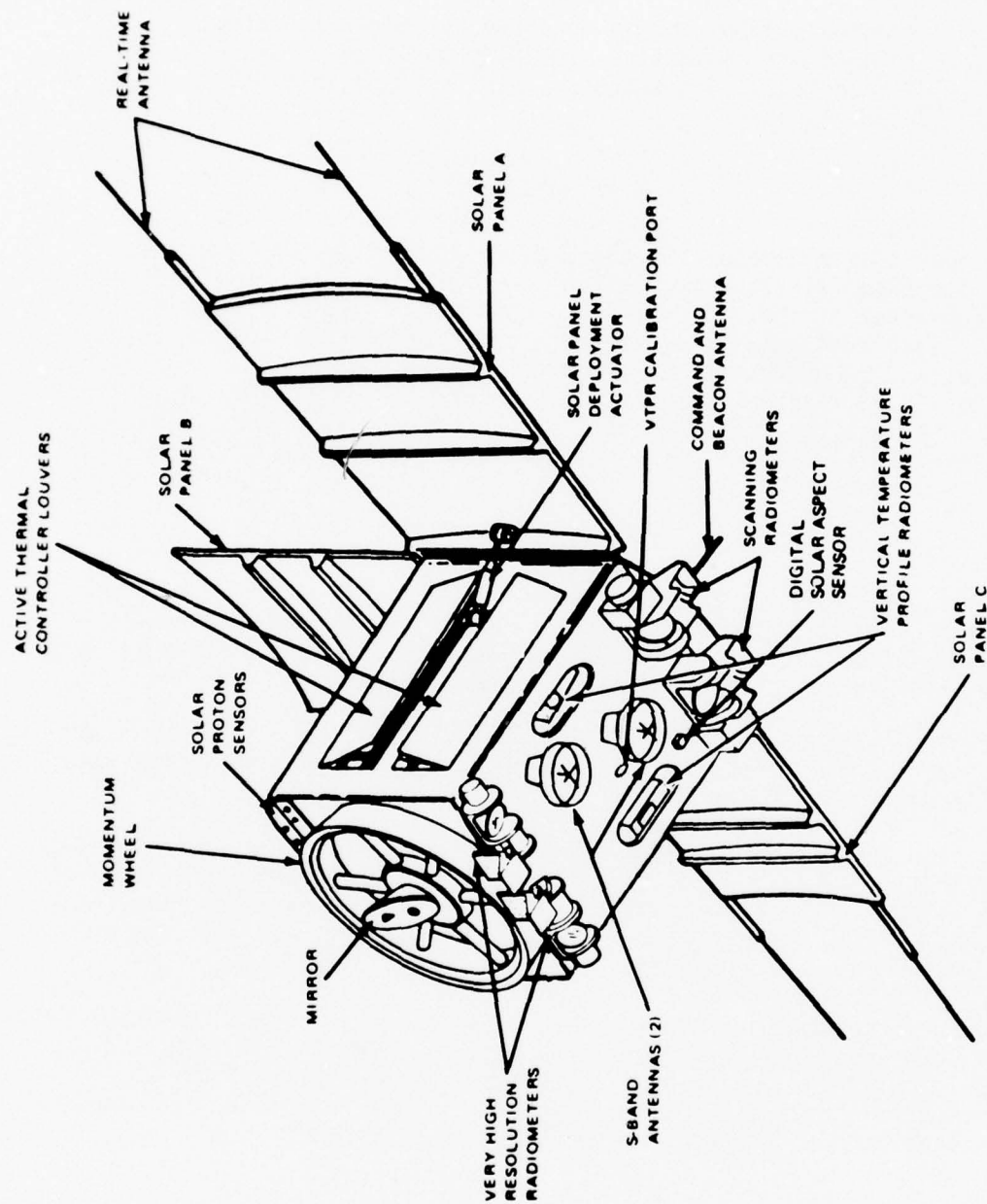


Figure 4. ITOS satellite.

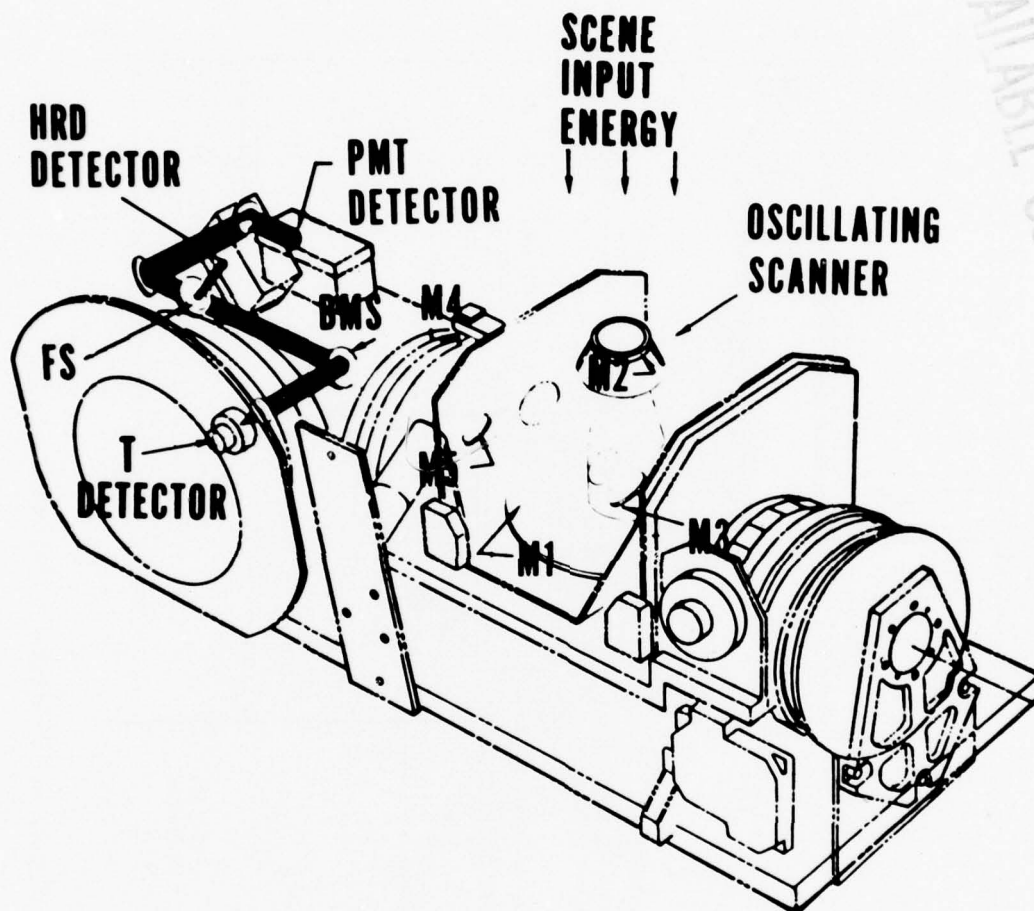
TABLE 3
ITOS-1 MAJOR OPERATING PARAMETERS

<u>Spacecraft Orbit</u>		<u>Scanning Radiometer</u>	
Orbit type	Sun-synchronous, circular, near-polar	Picture coverage	Continuous swath in direction of satellite travel. (Swath from horizon to horizon)
Altitude	790 nm	Channels	One IR channel - 10.5 μ m to 12.5 μ m One visible channel - 0.5 μ m to 0.73 μ m
Inclination	101.7° (78.3° retrograde)	Resolution	Visible - 2 nm IR - 4 nm
Period	115.2 min		
<u>APT Camera</u>		<u>AVCS TV Camera</u>	
Picture coverage	1800 by 1200 nm	Picture coverage per frame	1800 x 1800 nm
Picture overlap	20% in orbit track	Pictures per orbit and time	11 pictures - 44.2 min
Time per picture	158 sec	Picture interval	260 sec
TV lines per frame	600 lines	Picture overlap	50% in orbit track, 20% minimum in adjacent orbit
Picture interval	260 sec	Lens	f-1.8, 5.7mm focal length
No. of pictures	11	Field of view	108° across diagonal
Ground resolution	2 nm at local vertical	Line resolution	Approximately 800 TV lines
		Ground resolution	22 nm at local vertical
		Vidicon read time	6.25 sec
<u>AVCS Recorder</u>		<u>ITR</u>	
Storage capacity	33 pictures (3 orbits)	Record-incremental (stepper)	350 min (90 ft tape)
Record and playback tape speed	30 in./second	Record mode	15 bits/sec per track, 3 tracks-tape advance, 0.0033-in. increment, 15 times/sec
Playback time	2 min/orbit	Playback	162 sec
<u>Real-Time Link</u>			
Frequency	137.5 or 137.62 MHz (on alternate spacecraft)		
Transmitter power	5 W (minimum)		
Data	APT video, real-time SR video		

TABLE 4
SCANNER RESOLUTION IN NAUTICAL MILES
FOR THE DMSP BLOCK-5D SATELLITE

	<u>Visible</u>	<u>IR</u>
Day	0.3 x 0.3	0.3 x 0.3
Night	1.5 x 1.5	0.3 x 0.3

OLS - SENSING CONCEPT



M1, M2, M3, M4, M5 : PRIMARY
MIRRORS

BMS: BEAM SPLITTER; SPLITS INFARED ENERGY FROM VISIBLE ENERGY VIA MT1 AND MT2 (NOT SHOWN) TO THE T (THERMAL) DETECTOR.

FS : FIELD SPLITTER; SPLITS FIELD OF VIEW OF VISIBLE ENERGY FOR THE VISIBLE DETECTORS.

HRD: HIGH RESOLUTION DIODE (SMALL FIELD OF VIEW).

PMT: PHOTO MULTIPLIER TUBE (LARGER FIELD OF VIEW).

Figure 5. Operational linescan system.

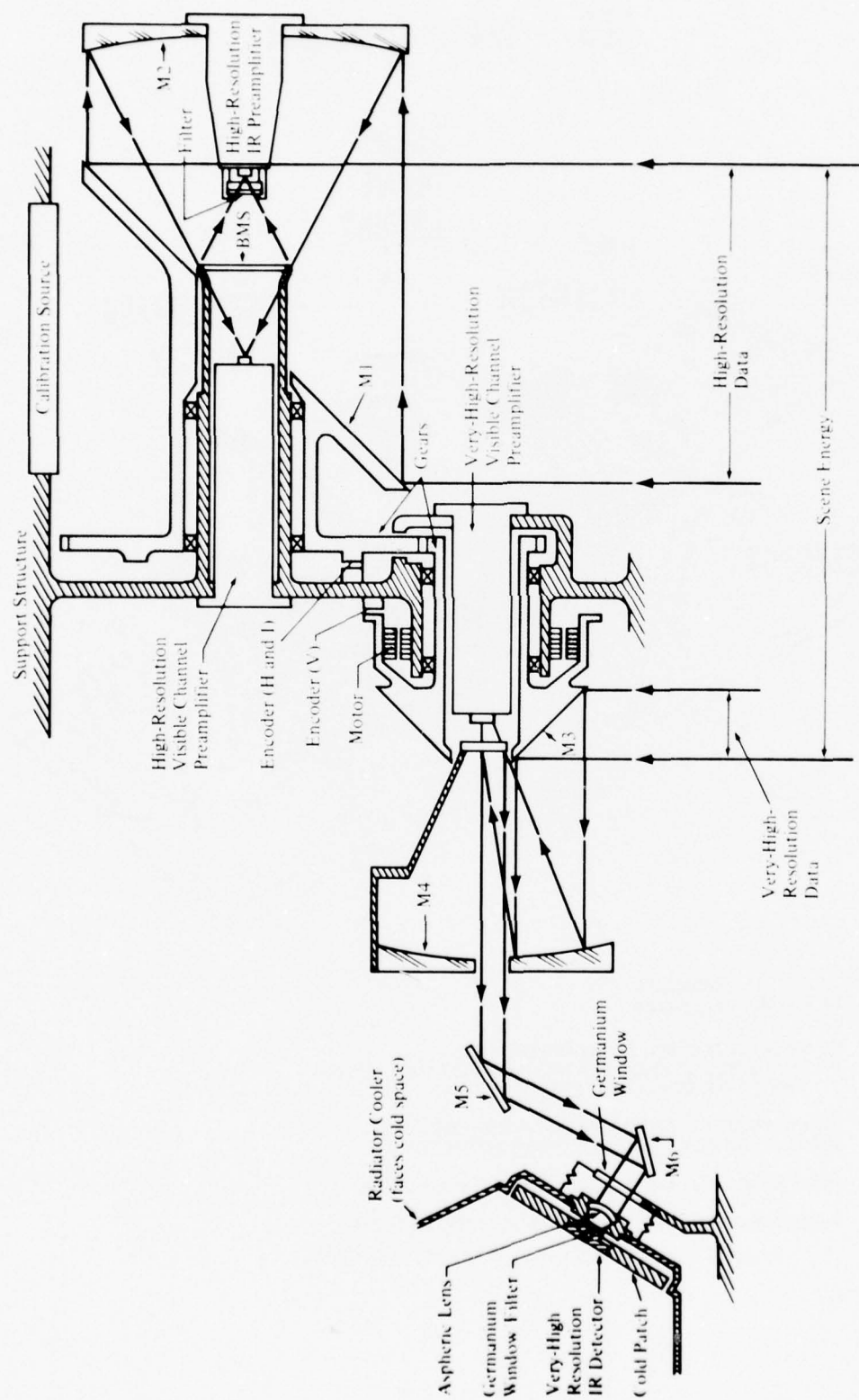


Figure 6. Radiometer instrument.

particles as well as from the gaseous constituents of the atmosphere. The matter which emits also absorbs at different narrow IR bands, thus causing attenuation in an atmospheric column which is undesirable in the determination of cloud-top temperature, particularly if the exact amount of absorbers is not known. Therefore, the narrow bands where the least amount of molecular or gaseous absorption exists need to be found. These narrow bands are commonly referred to as IR windows. There are two windows: one in the $3.7\mu\text{m}$ band and the other in the $10\mu\text{m}$ band. The former is not too well situated since some scattering by aerosol particles of solar radiation is appreciable at this wavelength. In the $10\mu\text{m}$ band, there is virtually no invasion of solar radiation, and the only absorber that needs to be considered is water vapor.

With the removal of solar energy from the radiative transfer equation (to be discussed in detail in a subsequent report), the radiance emerging from an emissive and scattering cloud of aerosol particles can be obtained by solving a much simpler transfer equation. Let N_λ be this spectral radiance and ϕ_λ the effective frequency response function. Then, the effective radiance \bar{N} to which an orbiting IR radiometer responds is given by

$$\bar{N} = \int_0^\infty N_\lambda \phi_\lambda d\lambda,$$

from which can be derived the so-called equivalent blackbody temperature of the body below. If the body is a cloud of liquid or solid aerosol particles, it is commonly considered the temperature of the cloud top. If the atmospheric column in the field of view of this radiometer is completely dry and free of any aerosol particles, the temperature is the equivalent surface temperature.

For this temperature of the cloud top to be of any real value in the determination of cloud-top height, as commonly practiced, it is important to investigate the conditions under which this equation may be valid. These conditions, pertinent remarks, and discussion of some solutions follow.

When an object radiates as a blackbody at a wavelength, its spectral emissivity is equal to unity; i.e., it is opaque to transmission at that frequency and nonreflecting. Depending upon the microphysical property, a cloud may or may not radiate like a blackbody at all wavelengths in the same IR window band. This phenomenon has been shown theoretically to be so by Shifrin [24], Yamamoto et al. [25], Zdunkowski and Choronenko [26], Yamamoto et al. [27], and Hunt [28].

Field observations by Gates and Shaw [29], Allen [30], Paltridge [31], and Platt and Bartusek [32] have also demonstrated a wide range of measured emissivities among different cloud types; unfortunately, none of these authors provided any microphysical data.

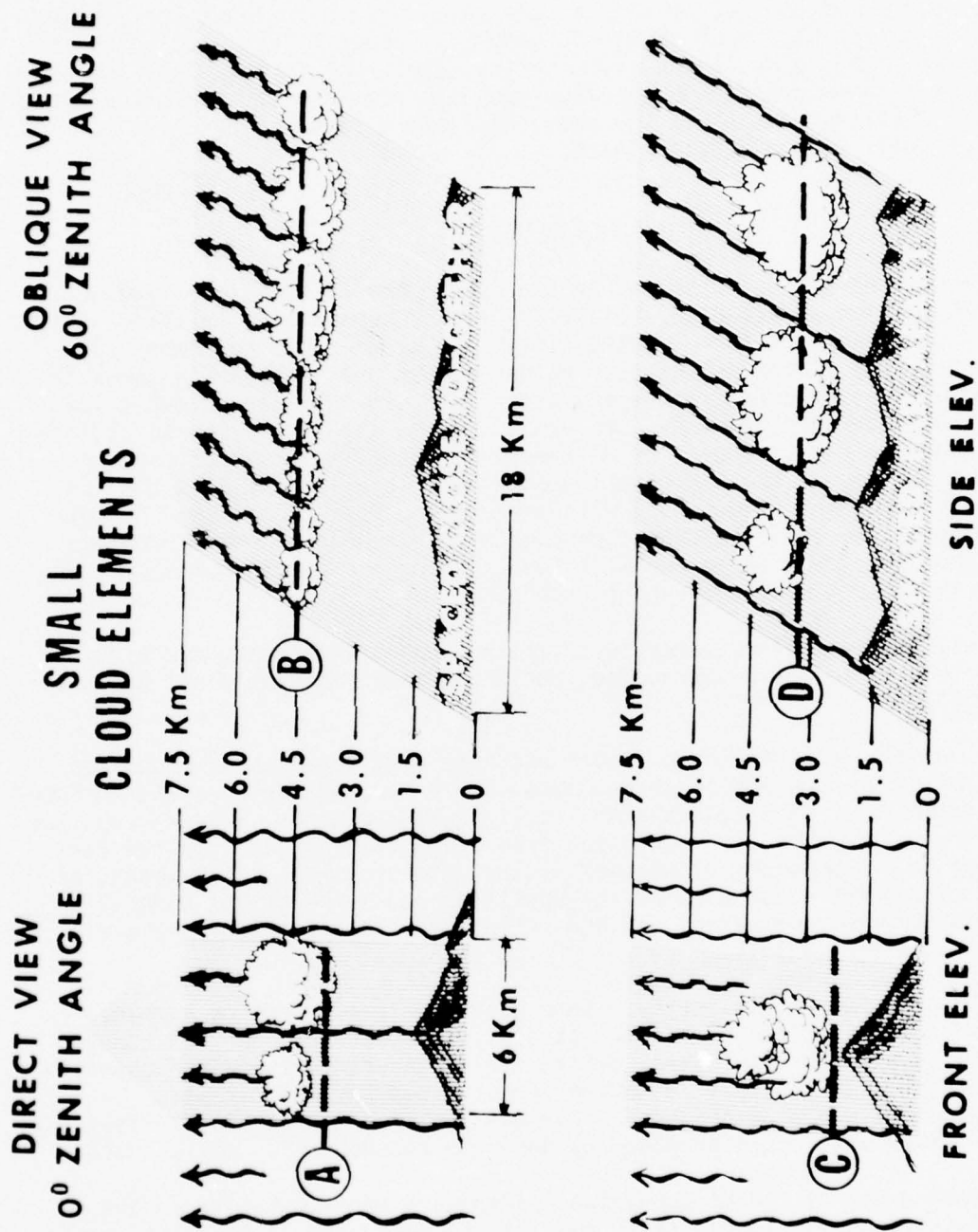
Next is the problem of the radiometer's field of view. Unless a cloud's areal expanse covers the field of view completely, the upwelling radiance reaching the radiometer will include ground radiation. As a result, the estimated cloud-top temperature will be higher and its estimated height correspondingly lower, if the vertical distribution of cloud temperature is a monotonically decreasing function of height.

The problems of scattered clouds and look angle may be included in this category. The latter is unique to SMS imagery since the satellite is parked at some longitude along the equator. The regions of interest to us generally lie somewhere in midlatitudes. Figure 7 (reproduced from an AWS technical report [33]) vividly illustrates these problems in the determination of cloud-top heights.

The radiometer may not respond equally to the wide range of thermal emission from the cloud and the ground surface; in other words, there may be greater errors in one temperature range than in another. There has been no known investigation of the response characteristics of the radiometers in the SMS under orbiting conditions. However, as an example, in the case of the earlier NOAA series, the IR radiometer showed an error ranging from $\pm 2^{\circ}\text{C}$ at the warm end of 300°K to $\pm 8^{\circ}\text{C}$ at the cold end of 185°K [33]. Anderson and Smith [33] estimated that with reference to the US Standard Atmosphere such errors would cause an uncertainty of about ± 300 m at the derived cloud-top height of 1000 m, about ± 600 m at 4200 m, about ± 1000 m at 7500 m, and about 1200 m at 10,000 m.

Also, cirrus clouds are present above the cloud deck of interest, and there may be several layers of clouds. As regards the former, both theoretical and experimental studies have been made of the optical properties of the cirrus cloud (e.g., [34-43]). The emissivity of the cirrus cloud varies from 0.1 to 0.75, depending upon its microstructure. Whether at the low end or the high end of emissivity, its presence causes an underestimate of the height of the lower cloud. Zdunkowski et al. [39] estimated that even invisible cirrus or haze could reduce the upwelling radiation by as much as 10%. The problem of multilayered clouds has been studied [44], but not to a great extent.

Gaseous constituents of the atmosphere exist also above the cloud. In the $10\mu\text{m}$ IR window, the absorbers are water vapor, carbon dioxide, and ozone; however, they apparently are not a problem since their amounts are rather small [45] above the cloud top.



The problem of the height-temperature relationship is least appreciated in the determination of cloud-top height. Though listed last here, this problem is by no means the least serious one. Unless the cloud is in complete thermodynamic equilibrium with its environment, i.e., the cloud and the environment share the same temperature lapse rate, the cloud-top height will become indeterminate.

SOME SOLUTIONS

Although the various problems in the use of the IR technique for the determination of cloud-top height are listed separately, it is convenient to discuss some of them together which may be amenable to common solutions. Some of the solutions considered here are necessarily somewhat speculative; however, such speculation is based on reasoned deduction. In the literature, most authors are concerned with the synoptic utilization of the cloud parameters derived from satellite observations. In general, these authors are satisfied with a knowledge of only the low, middle, and high clouds [46] with an error no less than ± 1 km in their height estimates. Therefore, they need only recognize these problems and not be overly concerned with them so long as the cloud information serves their global and synoptic purposes.

In military aviation, target acquisition, and severe storm tracking, an error of ± 1 km may be excessive, and these problems should not be taken lightly.

The problems pertaining to a more accurate determination of cloud-top height can be tackled in three ways: (a) extensive airborne and surface field observations, (b) in-situ satellite measurements, and (c) computer simulation of upwelling radiation from cloud atmospheres. In the last category are problems of whether a cloud radiates like a blackbody, of how the cirrus cloud affects the upwelling radiation of the underlying cloud and, to some extent, of how seriously an oblique look angle distorts radiance values.

Field experiments are costly. Some have been performed, as already noted above in cloud emissivity studies, but there are no firm conclusions in view of the rather limited field measurements and the observation cost. If a satellite had an unrestricted payload, in-situ measurement would be the best. For example, for cirrus cloud emissivity, the far-IR instrument proposed by Houghton and Hunt [47] may be used.

By making use of the microphysical parameters representative of the various types of clouds, it is possible to determine if the cloud having that type of microstructure radiates like a blackbody. However, warm and supercooled clouds should be modeled separately in view of the fact that the Mie scattering properties of water and ice particles are quite different. While the Mie parameters of spherical water droplets are fairly well-established, those of shaped ice crystals are not. Thus,

computer simulation of cirrus clouds would be somewhat difficult. There is an extreme paucity of microphysical data on the size and shape distribution of cirrus-type clouds; computer simulation of warm clouds would not be too difficult, and there is a relative abundance of microphysical data on various cloud types. Moreover, it may be feasible through numerical modeling to gain some knowledge of the apparent thickness of clouds. Once the cloud emissivity is known, it is relatively simple to calculate the temperature of the cloud top from the measured radiance.

Undoubtedly, an oblique look angle distorts the cloud picture. Unfortunately, the radiative transfer equation can only be solved efficiently for a plane parallel cloud although it is alleged that, in theory, the Monte Carlo technique will handle a cloud of any geometry. No literature has been found in this respect. On the other hand, the SMS parks at about 36,000 km above the equator; therefore, the look-angle distortion over the midlatitudes may not be too serious. Nevertheless, it would be advisable to make a comparative study of the cloud-top heights derived simultaneously over the same spot from both the SMS and the NOAA orbiter satellite. Because of angular obliquity, the correction factor to the SMS radiance values may well be a function of latitude. Once this correction factor is established, it may be applied to subsequent SMS radiance readings.

Scattered and multilayered clouds in the radiometer's field of view are problems of an entirely different category in which neither field nor satellite measurement would be of much help. For the former, computer simulation of randomly situated clouds appears to be the only solution. As to the latter, except for the case where the top cloud layer is thick enough to radiate like a blackbody, it would be difficult to simulate such clouds on a computer. Nazirov [48] used multilayered clouds to some advantage. He used the shadow of the top cloud cast upon the lower clouds as well as neighboring clouds to estimate the height of the top cloud.

The problem of instrument calibration or response error must also be considered. Since the satellite radiometers are calibrated onboard regularly, the assumption can be made that they are acceptable for purposes of this determination. However, it would be well-advised to check such calibration at the ground level to determine if there is any error at the warm ends as well as at the cold end and what correction, if any, needs to be applied.

SUMMATION

In this brief discussion of the problems and the solutions pertaining to the determination of cloud-top height, the authors have touched upon the technique in current use, the problems associated with this technique in

mesoscale applications, and the type of meteorological satellites required. Some solutions have also been offered. Presently, the synoptic meteorologists appear to be less concerned with certain ambiguities in their determination of cloud-top heights. As a matter of fact, the definition of cloud top, as quoted earlier from the Glossary of Meteorology is not in itself free from ambiguity. What can one say about the effect of different instruments?

Although, on the surface, it may not seem pertinent to the discussion here, it is nevertheless of interest to note a Russian study by Il'ina and Lapcheva [48] of the different techniques in their determination of cloud heights. They employed the satellite, the radiosonde and the radar for this purpose, and their findings are reproduced in Table 5.

Different sensors "interpret" the height of the cloud top in different ways, assuming no instrument errors. According to the table, the radiosonde gives the highest value; the radar, the middle value; and the satellite radiometer, the lowest. Herein lies the ambiguity of the instruments in use.

There has been no known effort in the meteorological community to extract cloud parameters from the SMS IR imagery. On the basis of past investigations, it may be safely stated that the cloud-top height is determined to no better than ± 1 km, using the orbiter satellites. With greater research effort in delineating the radiative properties of the clouds and the look angle problem, it appears to be entirely possible to refine our estimate of the cloud-top height to about ± 0.5 km for the case of total coverage in using the SMS alone.

On the other hand, for the case of scattered and multilayered clouds, the problems are more difficult. However, since it is not expected that cloud coverage 50% and less would greatly interfere with the Army's mesoscale operations, computer simulation may still be used to advantage. This problem will be tackled as soon as the problems associated with total coverage have been solved.

TABLE 5
COMPARISON OF CLOUD-TOP HEIGHTS OBTAINED BY THE PRESENT PROGRAM WITH
RADAR AND RADIOSONDE HEIGHTS FOR THE SUMMER OF 1970

Date	Time (hrs)		Orbit number	Cloud-top height H (km)				Difference (km)		Cloud form		Remarks
	satellite (sat)	radar (rad)		satellite	radar	sonde (son)		H _{sat} - H _{rad}	H _{sat} - H _{son}	satellite	ground stations	
13 July	1400	1410	261	2-3	5	4		-2	-1	☼ ☼ ☼ ☼	Cb, Ac, Ci	Cloudiness of secondary cold front
13 July	1400	1410	281	4-5	4	10		1	-5	☼ ☼ ☼ ☼	Ac, As, Ci	The same
7 Aug.	2020	1955	637	3-7	8	10		-1	-3	☼ ☼ ☼ ☼	Ac, Cu, Cb	Cloudiness of slow-moving front
7 Aug.	2020	1955	637	3-10	12	-		0	-	☼ ☼ ☼ ☼	Ac, As, Cu	ESSA-8 data as of 1139 hrs
23 Aug.	0759	740	940	2-4	3-4	8		0	-4	☼ ☼ ☼ ☼	Ac, As, Ci	Warm-front cloudiness
23 Aug.	0759	740	940	2-3	3-4	10		-1	-7	☼ ☼ ☼ ☼	Ac, As, Ci, Sc	The same
24 Sept.	1558	1553	1311	2-3	4	2		-1	1	☼ ☼ ☼ ☼	Cb, Ci, Cu, Ac	Cloudiness of secondary cold front
24 Sept.	1558	1553	1311	2-5	3	9		2	-4	☼ ☼ ☼ ☼	Cb, Ci, Cu, Ac	The same
24 Sept.	1553	1553	1311	2-3	3-4	8		-1	-5	☼ ☼ ☼ ☼	Cb, Ci, Cu, Sc	" "
26 Sept.	1533	1505	1338	2-4	4	6		0	-2	☼ ☼ ☼ ☼	Cb, Ac	" "
26 Sept.	1533	1505	1338	3-5	4	-		1	-	☼ ☼ ☼ ☼	Cb, Cu, Sc, Ac	" "
28 Sept.	1517	1528	1367	3-4	3	8		1	-4	☼ ☼ ☼ ☼	Cb, Cu, Ac, Ci	" "
$\Sigma \Delta H_{av}$								-1	-34			
$\Sigma 5 \text{ cases } \Delta H_{av}$								-0.1	-3			
								-6				
								-1				

ABBREVIATIONS

AFRCL	Air Force Cambridge Research Laboratories
ATS	Applications Technology Satellite
AWS	Air Weather Service
CDA	Command and Data Acquisition
DMSP	Defense Meteorological Satellite Program
DRGS	Direct Readout Ground Station
GOES	Geostationary Operational Environmental Satellite
IGFOV	Instantaneous geometric field of view
IR	Infrared
ITOS	Improved TIROS Operations System (TIROS = television and infrared observation satellite)
NETD	Noise equivalent temperature difference
NOAA	National Oceanic and Atmospheric Administration
OLS	Operational line-scan system
SATSEE	Satellite Target Visibility System
SATSTM	Severe Storm Observational System
SMS	Synchronous Meteorological Satellite
SR	Scanning radiometer
VAS	VISSR Atmospheric Sounder
VISSR	Visible Infrared Spin Scan Radiometer
VTPR	Vertical temperature profiling radiometer
WSMR	White Sands Missile Range

REFERENCES

1. Fritz, S. and J. S. Winston, 1962, "Synoptic Use of Radiation Measurements from Satellite TIROS II," Monthly Weather Rev., 90, 1-9.
2. Rasool, S. I., 1964, "Cloud Heights and Nighttime Cloud Cover From TIROS Radiation Data," J. Atmospheric Sci., 21, 152-156.
3. Saiedy, F., D. T. Hilleary, and W. A. Morgan, 1965, "Cloud Top Altitude Measurements From Satellites," Appl. Opt., 4, 495-500.
4. Rao, F. K. and J. S. Winston, 1963, "An Investigation of Some Synoptic Capabilities of Atmospheric 'Window' Measurements from Satellite TIROS II," J. Appl. Meteorol., 2, 12-33.
5. Koffler, R., A. G. DeCotiis, and P. K. Rao, 1973, "A Procedure for Estimating Cloud Amount and Height from Satellite Infrared Radiation Data," Monthly Weather Rev., 101, 240-243.
6. Boldyrev, V. G. and A. N. Katal'nikova, 1973, "Some Results of Determining Cloud Top Heights from Satellite Infrared Measurements," Advances in Satellite Meteorology, I, Israel Program for Scientific Translations (IPST), Jerusalem, 84-90.
7. Vonder Haar, T. H. and D. W. Reynolds, 1974, "A Bi-Spectral Method for Inferring Cloud Amount and Cloud-Top Temperature Using Satellite Data," Preprint, 6th Conf. Aeronautical Meteorol., 190-193.
8. Glahn, H. R., 1966, "On the Usefulness of Satellite Infrared Measurements in Determination of Cloud Top Heights and Areal Coverage," J. Appl. Meteorol., 5, 189-197.
9. Huschke, R. E., Ed., 1959, Glossary of Meteorology, American Meteorological Society, Boston, 638 pp.
10. Byers, H. R., 1959, General Meteorology, McGraw Hill, NY, 363-367.
11. Thomas, J. E., M. D. Kays, J. D. Horn, and R. L. Moore, 1975, "Visual Observation of Propagating Gravity Waves on ATS III Satellite Film Loops," ECOM-5553, Atmospheric Sciences Laboratory, White Sands Missile Range, NM.
12. Schwalb, A., "Modified Version of the Improved TIROS Operational Satellite (ITOS D-G)," NOAA Technical Memorandum NESS 35, National Environmental Satellite Service, NOAA, US Department of Commerce, Washington, D.C. (Apr 72).

13. McMillin, L. M. et al., 1973, "Satellite Infrared Sounding from NOAA Spacecraft," NOAA Technical Report Ness 65, Washington, D. C.
14. Nichols, D. A., 1975, "Block 5D-Compilation, January 1975," Defense Meteorological Satellite Program, SAMS0, USAF.
15. Dickinson, L. G., S. E. Boselly III, and W. S. Burgmann, "Defense Meteorological Satellite Program (DMSP) User's Guide," AWS-TR-74-250 (Dec 74).
16. Pipkin, F. B., "SMS System Description Document," Vol 11, GSFC, Greenbelt, MD (Oct 1971).
17. Abbott, T. M., Operational Manual: "Visible Infrared Spin Scan Radiometer (VISSR) for a Synchronous Meteorological Spacecraft (SMS)," Santa Barbara Research Center, Goleta, CA (Sep 73).
18. Shenk, W. E., Presentation at Conference on Satellite Studies of Severe Storms, the University of Texas at El Paso, Jun 75.
19. Duncan, Louis D., 1973, "A Geometric Investigation of the Effect of Viewing Angle on the Ground Resolution of Satellite-borne Sensors," ECOM-5502, Atmospheric Sciences Laboratory, White Sands Missile Range, NM
20. Maschoff, R., 1971, "Nimbus E Infrared Temperature Profile Radiometer ITPR Instrument Summary," Gulton Instrument Co.
21. Streaker, M. D., 1973, "The Nimbus F Observatory," ERTS-NIMBUS Proj., Off., Goddard Space Flight Center, Greenbelt, MD.
22. Chandrasekhar, S., 1960, Radiative Transfer, Dover, NY, 393.
23. Goody, R. M., 1964, Atmospheric Radiation, Oxford University Press, London, 436 pp.
24. Shifrin, K. S., 1950, "Spectral Properties of Clouds," Geofis. Pura. Appl., 48, 129-137.
25. Yamamoto, G., M. Tanaka, and K. Kamitani, 1966, "Radiative Transfer in Water Clouds in the 10- μ m Window Region," J. Atmospheric Sci., 23, 305-313.
26. Zdunkowski, W. G. and I. Choronenko, 1969, "Incomplete Blackness of Clouds in the Infrared Spectrum," Beitr. Atmos. Phys., 42, 206-224.

27. Yamamoto, G., M. Tanaka, and S. Asano, 1970, "Radiative Transfer in Water Clouds in the Infrared Region," J. Atmospheric Sci., 27, 282-292.
28. Hunt, G. E., 1973, "Radiative Properties of Terrestrial Clouds at Visible and Infrared Thermal Window Wavelength," Quart. J. Roy. Meteorol. Soc., 99, 346-369.
29. Gates, D. M. and C. C. Shaw, 1960, "Infrared Transmission of Clouds," J. Opt. Soc. Am., 50, 876-882.
30. Allen, J. R., 1971, "Measurements of Cloud Emissivity in the 8-13 μ m Waveband," J. Appl. Meteorol., 10, 260-265.
31. Paltridge, G. W., 1974, "Infrared Emissivity, Short-wave Albedo, and the Microphysics of Stratiform Water Clouds," J. Geophys. Res., 79, 4053-4058.
32. Platt, C. M. R. and K. Bartusek, 1974, "Structure and Optical Properties of Some Middle-level Clouds," J. Atmospheric Sci., 31, 1079-1088.
33. Anderson, R. K. and A. H. Smith, 1971, "Application of Meteorological Satellite Data in Analysis and Forecasting," AWS Tech Rpt 212, USAF Air Weather Service.
34. Kuhn, P. M., 1963, "Measured Effective Long-wave Emissivity of Clouds," Monthly Weather Rev., 91, 12-18.
35. Platt, C. M. R. and D. J. Gambling, 1971, "Emissivity of High Layer Clouds by Combined Lidar and Radiometric Techniques," Quart. J. Roy. Meteorol. Soc., 97, 322-325.
36. Platt, C. M. R., 1972, "Airborne Infrared Radiance Measurements (10-12 μ m) Off Tropical East-Coast Australia," J. Geophys. Res., 77, 1597-1609.
37. Platt, C. M. R., 1973, "Lidar and Radiometer Observations of Cirrus Clouds," J. Atmospheric Sci., 30, 1191-1204.
38. Valovcin, F. R., 1968, "Infrared Measurements of Jet-Stream Cirrus," J. Appl. Meteorol., 7, 817-826.
39. Zdunkowski, W. G., D. Henderson, and J. V. Hales, 1965, "The Influence of Haze on Infrared Radiation Measurements Detected by Space Vehicles," Tellus, 17, 147-165.

40. Fritz, S. and P. K. Rao, 1967, "On the Infrared Transmission Through Cirrus Clouds and the Estimation of Relative Humidity from Satellites," J. Appl. Meteorol., 6, 1088-1096.
41. Liou, K. N., 1972, "Light Scattering by Ice Clouds in the Visible and Infrared: A Theoretical Study," J. Atmospheric Sci., 29, 524-536.
42. Liou, K. N., 1973, "Transfer of Solar Irradiance Through Cirrus Cloud Layers," J. Geophys. Res., 78, 1409-1418.
43. Liou, K. N., 1974, "On the Radiative Properties of Cirrus in the Window Region and Their Influence on Remote Sensing of the Atmosphere," J. Atmospheric Sci., 31, 522-532.
44. Cooley, D. S., J. T. Ball, and A. M. Pavlowitz, 1970, "Layered Cloud Analyses Derived from Satellite and Conventional Data," J. Appl. Meteorol., 9, 158-169.
45. Shenk, W. E. and V. V. Salomonson, 1970, "Visible and Infrared Imagery From Meteorological Satellites," Appl. Opt., 9, 1747-1760.
46. Rao, F. K., 1970, "Estimating Cloud Amount and Height from Satellite Infrared Radiation Data," ESSA Tech. Rpt. NESC 54, 11 pp.
47. Houghton, J. T. and G. E. Hunt, 1971, "The Detection of Ice Clouds From Remote Measurements of Their Emission in the Far Infrared," Quart. J. Roy. Meteorol. Soc.
48. Nazirov, M., 1970, "Shadow on Satellite Photographs as a Source of Information on the Height of Clouds," Problems of Satellite Meteorology, IPST, Jerusalem, 20-25.
49. Il'ina, G. I. and V. F. Papcheva, 1973, "Comparison of Satellite Measured and Radar-Observed Cloud-Top Heights," Advances in Satellite Meteorology, I, IPST, Jerusalem, 145-153.

ATMOSPHERIC SCIENCES RESEARCH PAPERS

1. Lindberg, J.D., "An Improvement to a Method for Measuring the Absorption Coefficient of Atmospheric Dust and other Strongly Absorbing Powders," ECOM-5565, July 1975.
2. Avara, Elton, P., "Mesoscale Wind Shears Derived from Thermal Winds," ECOM-5566, July 1975.
3. Gomez, Richard B. and Joseph H. Pierluissi, "Incomplete Gamma Function Approximation for King's Strong-Line Transmittance Model," ECOM-5567, July 1975.
4. Blanco, A.J. and B.F. Engebos, "Ballistic Wind Weighting Functions for Tank Projectiles," ECOM-5568, August 1975.
5. Taylor, Fredrick J., Jack Smith, and Thomas H. Pries, "Crosswind Measurements through Pattern Recognition Techniques," ECOM-5569, July 1975.
6. Walters, D.L., "Crosswind Weighting Functions for Direct-Fire Projectiles," ECOM-5570, August 1975.
7. Duncan, Louis D., "An Improved Algorithm for the Iterated Minimal Information Solution for Remote Sounding of Temperature," ECOM-5571, August 1975.
8. Robbiani, Raymond L., "Tactical Field Demonstration of Mobile Weather Radar Set AN/TPS-41 at Fort Rucker, Alabama," ECOM-5572, August 1975.
9. Miers, B., G. Blackman, D. Langer, and N. Lorimier, "Analysis of SMS/GOES Film Data," ECOM-5573, September 1975.
10. Manquero, Carlos, Louis Duncan, and Rufus Bruce, "An Indication from Satellite Measurements of Atmospheric CO₂ Variability," ECOM-5574, September 1975.
11. Petracca, Carmine and James D. Lindberg, "Installation and Operation of an Atmospheric Particulate Collector," ECOM-5575, September 1975.
12. Avara, Elton P. and George Alexander, "Empirical Investigation of Three Iterative Methods for Inverting the Radiative Transfer Equation," ECOM-5576, October 1975.
13. Alexander, George D., "A Digital Data Acquisition Interface for the SMS Direct Readout Ground Station—Concept and Preliminary Design," ECOM-5577, October 1975.
14. Cantor, Israel, "Enhancement of Point Source Thermal Radiation Under Clouds in a Nonattenuating Medium," ECOM-5578, October 1975.
15. Norton, Colburn and Glenn Hoidale, "The Diurnal Variation of Mixing Height by Month over White Sands Missile Range, NM," ECOM-5579, November 1975.
16. Avara, Elton P., "On the Spectrum Analysis of Binary Data," ECOM-5580, November 1975.
17. Taylor, Fredrick J., Thomas H. Pries, and Chao-Huan Huang, "Optimal Wind Velocity Estimation," ECOM-5581, December 1975.
18. Avara, Elton P., "Some Effects of Autocorrelated and Cross-Correlated Noise on the Analysis of Variance," ECOM-5582, December 1975.
19. Gillespie, Patti S., R.L. Armstrong, and Kenneth O. White, "The Spectral Characteristics and Atmospheric CO₂ Absorption of the Ho⁺:YLF Laser at 2.05 μ m," ECOM-5583, December 1975.
20. Novlan, David J., "An Empirical Method of Forecasting Thunderstorms for the White Sands Missile Range," ECOM-5584, February 1976.
21. Avara, Elton P., "Randomization Effects in Hypothesis Testing with Autocorrelated Noise," ECOM-5585, February 1976.
22. Watkins, Wendell R., "Improvements in Long Path Absorption Cell Measurement," ECOM-5586, March 1976.
23. Thomas, Joe, George D. Alexander, and Marvin Dubbin, "SATTEL — An Army Dedicated Meteorological Telemetry System," ECOM-5587, March 1976.
24. Kennedy, Bruce W. and Delbert Bynum, "Army User Test Program for the RDT&E-XM-75

25. Barnett, Kenneth M., "A Description of the Artillery Meteorological Comparisons at White Sands Missile Range, October 1974 - December 1974 ('PASS' - Prototype Artillery [Meteorological] Subsystem)," ECOM-5589, April 1976.
26. Miller, Walter B., "Preliminary Analysis of Fall-of-Shot From Project 'PASS'," ECOM-5590, April 1976.
27. Avara, Elton P., "Error Analysis of Minimum Information and Smith's Direct Methods for Inverting the Radiative Transfer Equation," ECOM-5591, April 1976.
28. Yee, Young P., James D. Horn, and George Alexander, "Synoptic Thermal Wind Calculations from Radiosonde Observations Over the Southwestern United States," ECOM-5592, May 1976.
29. Duncan, Louis D. and Mary Ann Seagraves, "Applications of Empirical Corrections to NOAA-4 VTPR Observations," ECOM-5593, May 1976.
30. Miers, Bruce T. and Steve Weaver, "Applications of Meteorological Satellite Data to Weather Sensitive Army Operations," ECOM-5594, May 1976.
31. Sharenow, Moses, "Redesign and Improvement of Balloon ML-566," ECOM-5595, June 1976.
32. Hansen, Frank V., "The Depth of the Surface Boundary Layer," ECOM-5596, June 1976.
33. Pinnick, R.G. and E.B. Stenmark, "Response Calculations for a Commercial Light-Scattering Aerosol Counter," ECOM-5597, July 1976.
34. Mason, J. and G.B. Hoidale, "Visibility as an Estimator of Infrared Transmittance," ECOM-5598, July 1976.
35. Bruce, Rufus E., Louis D. Duncan, and Joseph H. Pierluissi, "Experimental Study of the Relationship Between Radiosonde Temperatures and Radiometric-Area Temperatures," ECOM-5599, August 1976.
36. Duncan, Louis D., "Stratospheric Wind Shear Computed from Satellite Thermal Sounder Measurements," ECOM-5800, September 1976.
37. Taylor, F., P. Mohan, P. Joseph and T. Pries, "An All Digital Automated Wind Measurement System," ECOM-5801, September 1976.
38. Bruce, Charles, "Development of Spectrophones for CW and Pulsed Radiation Sources," ECOM-5802, September 1976.
39. Duncan, Louis D. and Mary Ann Seagraves, "Another Method for Estimating Clear Column Radiances," ECOM-5803, October 1976.
40. Blanco, Abel J. and Larry E. Traylor, "Artillery Meteorological Analysis of Project Pass," ECOM-5804, October 1976.
41. Miller, Walter and Bernard Engebos, "A Mathematical Structure for Refinement of Sound Ranging Estimates," ECOM-5805, November, 1976.
42. Gillespie, James B. and James D. Lindberg, "A Method to Obtain Diffuse Reflectance Measurements from 1.0 to 3.0 μm Using a Cary 17I Spectrophotometer," ECOM-5806, November 1976.
43. Rubio, Roberto and Robert O. Olsen, "A Study of the Effects of Temperature Variations on Radio Wave Absorption," ECOM-5807, November 1976.
44. Ballard, Harold N., "Temperature Measurements in the Stratosphere from Balloon-Borne Instrument Platforms, 1968-1975," ECOM-5808, December, 1976.
45. Monahan, H.H., "An Approach to the Short-Range Prediction of Early Morning Radiation Fog," ECOM-5809, January 1977.
46. Engebos, Bernard Francis, "Introduction to Multiple State Multiple Action Decision Theory and Its Relation to Mixing Structures," ECOM-5810, January 1977.
47. Low, Richard D.H., "Effects of Cloud Particles on Remote Sensing from Space in the 10-Micrometer Infrared Region," ECOM-5811, January 1977.
48. Bonner, Robert S. and R. Newton, "Application of the AN/GVS-5 Laser Rangefinder to Cloud Base Height Measurements," ECOM-5812, February 1977.

49. Rubio, Roberto, "Lidar Detection of Subvisible Reentry Vehicle Erosive Atmospheric Material," ECOM-5813, March 1977.
50. Low, Richard D.H. and J.D. Horn, "Mesoscale Determination of Cloud-Top Height: Problems and Solutions," ECOM-5814, March 1977.

DISTRIBUTION LIST

Commanding Officer
Picatinny Arsenal
ATTN: SARPA-TS-S, #59
Dover, NJ 07801

Commanding Officer
Harry Diamond Laboratory
ATTN: Library
2800 Powder Mill Road
Adelphi, MD 20783

Commander
US Army Electronics Command
ATTN: DRSEL-RD-D
Fort Monmouth, NJ 07703

Naval Surface Weapons Center
Code DT 21 (Ms. Greeley)
Dahlgren, VA 22448

Air Force Weapons Laboratory
ATTN: Technical Library (SUL)
Kirtland AFB, NM 87117

Director
US Army Engr Waterways Exper Sta
ATTN: Library Branch
Vicksburg, MS 39180

Commander
US Army Electronics Command
ATTN: DRSEL-CT-D
Fort Monmouth, NJ 07703

Meteorologist in Charge
Kwajalein Missile Range
PO Box 67
APO
San Francisco, CA 96555

Environmental Protection Agency
Meteorology Laboratory
Research Triangle Park, NC 27711

Chief, Technical Services Div
DCS/Aerospace Sciences
ATTN: AWS/DNTI
Scott AFB, IL 62225

Air Force Cambridge Rsch Labs
ATTN: LCH (A. S. Carten, Jr.)
Hanscom AFB
Bedford, MA 01731

Department of the Air Force
16WS/D0
Fort Monroe, VA 23651

Director
US Army Ballistic Research Lab
ATTN: DRXBR-AM
Aberdeen Proving Ground, MD 21005

Geophysics Division
Code 3250
Pacific Missile Test Center
Point Mugu, CA 93042

National Center for Atmos Res
NCAR Library
PO Box 3000
Boulder, CO 80303

William Peterson
Research Association
Utah State University, UNC 48
Logan, UT 84322

Commander
US Army Dugway Proving Ground
ATTN: MT-S
Dugway, UT 84022

Head, Rsch and Development Div (ESA-131)
Meteorological Department
Naval Weapons Engineering Support Act
Washington, DC 20374

Commander
US Army Electronics Command
ATTN: DRCDE-R
5001 Eisenhower Avenue
Alexandria, VA 22304

Marine Corps Dev & Educ Cmd
Development Center
ATTN: Cmd, Control, & Comm Div (C³)
Quantico, VA 22134

Commander
US Army Electronics Command
ATTN: DRSEL-WL-D1
Fort Monmouth, NJ 07703

Commander
US Army Missile Command
ATTN: DRSMI-RFGA, B. W. Fowler
Redstone Arsenal, AL 35809

Dir of Dev & Engr
Defense Systems Div
ATTN: SAREA-DE-DDR
H. Tannenbaum
Edgewood Arsenal, APG, MD 21010

Mr. William A. Main
USDA Forest Service
1407 S. Harrison Road
East Lansing, MI 48823

Naval Surface Weapons Center
Technical Library and Information
Services Division
White Oak, Silver Spring, MD 20910

Dr. A. D. Belmont
Research Division
PO Box 1249
Control Data Corp
Minneapolis, MN 55440

Dir, Elec Tech and Devices Lab
US Army Electronics Command
ATTN: DRSEL-TL-D, Bldg 2700
Fort Monmouth, NJ 07703

Director
Development Center MCDEC
ATTN: Firepower Division
Quantico, VA 22134

Commander
US Army Proving Ground
ATTN: Technical Library, Bldg 2100
Yuma, AZ 85364

US Army Liaison Office
MIT-Lincoln Lab, Library A-082
PO Box 73
Lexington, MA 02173

Library-R-51-Tech Reports
Environmental Research Labs
NOAA
Boulder, CO 80302

Head, Atmospheric Research Section
National Science Foundation
1800 G. Street, NW
Washington, DC 20550

Commander
US Army Missile Command
ATTN: DRSMI-RR
Redstone Arsenal, AL 35809

Commandant
US Army Field Artillery School
ATTN: Met Division
Fort Sill, OK 73503

Meteorology Laboratory
AFCRL/LY
Hanscom AFB
Bedford, MA 01731

Commander
US Army Engineer Topographic Lab
(STINFO CENTER)
Fort Belvoir, VA 22060

Commander
US Army Missile Command
ATTN: DRSMI-RRR, Bldg 7770
Redstone Arsenal, AL 35809

Air Force Avionics Lab
ATTN: AFAL/TSR
Wright-Patterson AFB, Ohio 45433

Commander
US Army Electronics Command
ATTN: DRSEL-VL-D
Fort Monmouth, NJ 07703

Commander
USAICS
ATTN: ATSI-CTD-MS
Fort Huachuca, AZ 85613

EXR Center
Bureau of Reclamation
ATTN: Bldg 67, Code 1210
Denver, CO 80225

HQDA (DAEN-RDM/Dr. De Percin)
Forrestal Bldg
Washington, DC 20314

Commander
Air Force Weapons Laboratory
ATTN: AFWL/WE
Kirtland AFB, NM 87117

Commander
US Army Satellite Comm Agc
ATTN: DRCPM-SC-3
Fort Monmouth, NJ 07703

Commander
US Army Electronics Command
ATTN: DRSEL-MS-TI
Fort Monmouth, NJ 07703

Commander
US Army Electronics Command
ATTN: DRSEL-GG-TD
Fort Monmouth, NJ 07703

Dr. Robert Durrenberger
Dir, The Lab of Climatology
Arizona State University
Tempe, AZ 85281

Commander
Headquarters, Fort Huachuca
ATTN: Tech Ref Div
Fort Huachuca, AZ 85613

Field Artillery Consultants
1112 Becontree Drive
ATTN: COL Buntyn
Lawton, OK 73501

Commander
US Army Nuclear Agency
ATTN: ATCA-NAW
Building 12
Fort Bliss, TX 79916

Director
Atmospheric Physics & Chem Lab
Code 31, NOAA
Department of Commerce
Boulder, CO 80302

Dr. John L. Walsh
Code 5503
Navy Research Lab
Washington, DC 20375

Commander
US Army Air Defense School
ATTN: C&S Dept, MSLSCI Div
Fort Bliss, TX 79916

Director National Security Agency
ATTN: TDL (C513)
Fort George G. Meade, MD 20755

USAF EPAC/CBT (Stop 825)
ATTN: Mr. Burgmann
Scott AFB, IL 62225

Armament Dev & Test Center
ADTC (DLOSL)
Eglin AFB, Florida 32542

Commander
US Army Ballistic Rsch Labs
ATTN: DRXBR-IB
Aberdeen Proving Ground, MD 21005

Director
Naval Research Laboratory
Code 2627
Washington, DC 20375

Commander
Naval Elect Sys Cmd HQ
Code 51014
Washington, DC 20360

The Library of Congress
ATTN: Exchange & Gift Div
Washington, DC 20540
2

CO, US Army Tropic Test Center
ATTN: STETC-MO-A (Tech Lib)
APO New York 09827

Commander
Naval Electronics Lab Center
ATTN: Library
San Diego, CA 92152

Office, Asst Sec Army (R&D)
ATTN: Dep for Science & Tech
Hq, Department of the Army
Washington, DC 20310

Director
US Army Ballistic Research Lab
ATTN: DRXBR-AM, Dr. F. E. Niles
Aberdeen Proving Ground, MD 21005

Commander
Frankford Arsenal
ATTN: Library, K2400, Bldg 51-2
Philadelphia, PA 19137

Director
US Army Ballistic Research Lab
ATTN: DRXBR-XA-LB
Bldg 305
Aberdeen Proving Ground, MD 21005

Dir, US Naval Research Lab
Code 5530
Washington, DC 20375

Commander
Office of Naval Research
Code 460-M
Arlington, VA 22217

Commander
Naval Weather Service Command
Washington Navy Yard
Bldg 200, Code 304
Washington, DC 20374

Technical Processes Br
DS23
Room 806, Libraries Div NOAA
8060 13th St
Silver Spring, MD 20910

The Environmental Rsch Institute of MI
ATTN: IRIA Library
PO Box 618
Ann Arbor, MI 48107

Redstone Scientific Info Center
ATTN: Chief, Documents
US Army Missile Command
Redstone Arsenal, AL 35809

Commander
Edgewood Arsenal
ATTN: SAREA-TS-L
Aberdeen Proving Ground, MD 21010

Sylvania Elec Sys Western Div
ATTN: Technical Reports Library
PO Box 205
Mountain View, CA 94040

Commander
US Army Security Agency
ATTN: IARD-OS
Arlington Hall Station
Arlington, VA 22212
2

President
US Army Field Artillery Board
Fort Sill, OK 73503

Commandant
US Army Field Artillery School
ATTN: ATSF-TA-R
Fort Sill, OK 73503

CO, USA Foreign Sci & Tech Center
ATTN: DRXST-ISI
220 7th Street, NE
Charlottesville, VA 22901

Commander, Naval Ship Sys Cmd
Technical Library, Rm 3 S-08
National Center No. 3
Washington, DC 20360

Commandant
US Army Signal School
ATTN: ATSN-CD-MS
Fort Gordon, GA 30905

Rome Air Development Center
ATTN: Documents Library
TILD (Bette Smith)
Griffiss Air Force Base, NY 13441

HQ, ESD/DRI/S-22
Hanscom AFB
MA 01731

Commander
Frankford Arsenal
ATTN: J. Helfrich PDSP 65-1
Philadelphia, PA 19137

Director
Defense Nuclear Agency
ATTN: Tech Library
Washington, DC 20305

Department of the Air Force
5WW/DOX
Langley AFB, VA 23665

Commander
US Army Missile Command
ATTN: DRSMI-RER (Mr. Haraway)
Redstone Arsenal, AL 35809

CPT Hugh Albers, Exec Sec
Interdept Committee on Atmos Sci
Fed Council for Sci & Tech
National Sci Foundation
Washington, DC 20550

US Army Research Office
ATTN: DRXRO-IP
PO Box 12211
Research Triangle Park, NC 27709

Dr. Frank D. Eaton
PO Box 3038
University Station
Laramie, Wyoming 82071

Commander
US Army Training & Doctrine Cmd
ATTN: ATCD-SC
Fort Monroe, VA 23651

Commander
US Army Arctic Test Center
ATTN: STEAC-OP-PL
APO Seattle 98733

Mil Assistant for Environmental Sciences
OAD (E & LS), 3D129
The Pentagon
Washington, DC 20301

Commander
US Army Electronics Command
ATTN: DRSEL-GS-H (Stevenson)
Fort Monmouth, NJ 07703

Commander
Eustis Directorate
US Army Air Mobility R&D Lab
ATTN: Technical Library
Fort Eustis, VA 23604

Commander
USACACDA
ATTN: ATCA-CCC-W
Fort Leavenworth, KS 66027

National Weather Service
National Meteorological Center
World Weather Bldg - 5200 Auth Rd
ATTN: Mr. Quiroz
Washington, DC 20233

Commander
US Army Test & Eval Cmd
ATTN: DRSTE-FA
Aberdeen Proving Ground, MD 21005

Commander
US Army Materiel Command
ATTN: DRCRD-SS (Mr. Andrew)
Alexandria, VA 22304

Air Force Cambridge Rsch Labs
ATTN: LKI
L. G. Hanscom Field
Bedford, MA 01730

Commander
Frankford Arsenal
ATTN: SARFA-FCD-O, Bldg 201-2
Bridge & Tarcony Sts
Philadelphia, PA 19137

Director, Systems R&D Service
Federal Aviation Administration
ATTN: ARD-54
2100 Second Street, SW
Washington, DC 20590

Inge Dirmhirn, Professor
Utah State University, UMC 48
Logan, UT 84322

USAFETAC/CB (Stop 825)
Scott AFB
IL 62225

Chief, Aerospace Environ Div
Code ES41
NASA
Marshall Space Flight Center, AL 35802

Director
USAE Waterways Experiment Station
ATTN: Library
PO Box 631
Vicksburg, MS 39180

Defense Documentation Center
ATTN: DDC-TCA
Cameron Station (BLDG 5)
Alexandria, Virginia 22314
12

Commander
US Army Electronics Command
ATTN: DRSEL-CT-S
Fort Monmouth, NJ 07703

Commander
Holloman Air Force Base
6585 TG/WE
Holloman AFB, NM 88330

Commandant
USAFAS
ATTN: ATSF-CD-MT (Mr. Farmer)
Fort Sill, OK 73503
2

Commandant
USAFAS
ATTN: ATSF-CD-C (Mr. Shelton)
Fort Sill, OK 73503
2

Commander
US Army Electronics Command
ATTN: DRSEL-CT-S (Dr. Swingle)
Fort Monmouth, NJ 07703
3